World Journal of Applied Chemistry
2024, Vol. 9, No. 3, pp. 44-55
https://doi.org/10.11648/j.wjac.20240903.12

Research Article

Adsorption of Iron (II) from Aqueous Solution by Activated Carbon from Desert Date Seed Shells (*Balanites Aegyptiaca*)

Dani de Benessoubo Kada[1], Domga[2,*], Celestine Yanu Asobo[3], Ngaba Taybe[4], Jean Olivier Kowe[5]

[1]Department of Chemical Engineering, University Institute of Technology, The University of Ngaoundere, Ngaoundere, Cameroun

[2]Department of Chemical Engineering, School of Chemical Engineering and Mineral Industries (EGCIM), The University of Ngaoundere, Ngaoundere, Cameroon

[3]Department of Chemistry, Faculty of Science, The University of Buea, Buea, Cameroon

[4]Departement of Civil Engineering and Architecture, National Advanced School of Engineering, The University of Maroua, Maroua, Cameroon

[5]Department of Chemistry, Faculty of Science, The University of Ngaoundere, Ngaoundere, Cameroon

Abstract

The presence of heavy metals in water is one of the major environmental issues. In this study, desert date seed shells were employed as precursors for the production of activated carbon by chemical activation process using phosphoric acid (DDSSA) and potassium hydroxide (DDSSS). The activated carbon derived desert date seed were characterized using XRD, FTIR, Raman spectroscopy, SEM analysis and point of zero charge. The most significant variables that affect the adsorption of iron ions, including pH, contact time, and initial concentration, have been investigated. The results of the research were successfully assessed by Langmuir model. Interestingly, the maximum adsorption ability of Fe^{2+} was found to be 132.25 mg/g onto DDSSA and 126.35 mg/g onto DDSSS, this was found to be higher in comparison to the similar activated carbon obtained by other researchers. The pseudo 2^{nd} order model was also utilized to describe the adsorption and the data showed that adsorption kinetic of Fe^{2+} ions onto the DDSSA and DDSSS is dominated by chemisorption. Moreover, thermodynamic parameters suggested that DDSSA and DDSSS for Fe (II) adsorption phenomenon were endothermic and spontaneous. Taken together the high availability, facile production along with high performance of activated carbon from desert date seed shells make it an economically adsorbent for Fe (II) adsorption.

Keywords

Adsorbents, Activated Carbon, Water Treatment, Isotherm, Iron, Desert Date Seed Shells

[*]Corresponding author: tdomga@yahoo.fr (Domga)

Received: 13 July 2024; **Accepted:** 5 August 2024; **Published:** 15 August 2024

1. Introduction

One of the main potential risks to humanity is water pollution, which is a result of rapid industrialization and urbanization. Contamination of water affects all living organisms, communities, and aquatic ecosystems. Because it is so difficult to remove heavy metals from the water system, they are considered to be among the most harmful of the several aquatic pollutants [1, 2]. Heavy metals are widely used in various industries, including leather, petrochemical, metal plating, agriculture, municipal wastewater treatment, paper and pulp, and other environmental fields.

Because of the possible effects on human health, the goal of environmental study has been heavily concentrated on wastewater from industry or municipalities. Different harmful heavy metals, including arsenic, iron, zinc, cadmium, mercury, silver, lead, copper, and the platinum group elements, are present in industrial and municipal wastewater [3-5]. Dirt and water pollution results from discharging these materials into the ecosystem. Making up over 5.63 percent of the earth's crust, iron is the most abundant metal among those listed above [5].

Most common and plentiful materials have iron ions, including those utilized in smelting processes, agrochemicals, mining, the electronic industries, transportation, mechanical manufacturing sector, industry units, and architecture [6, 7]. Low iron concentration can be found in all natural water sources [8]. However, due to leaching from the pipes, the concentration of this component may rise if drinkable water sits in iron household pipes for an extended period of time. Iron is essential to human health, but at excessive concentrations, it can have harmful effects just like other heavy metal ions. The World Health Organization (WHO) advises the maximum allowable limit of iron concentration in consumable water is 0.3 mg/L [8, 9]. Being poisonous and non-biodegradable, an increase in the amount of this metal in the water poses a serious threat to humankind. In fact, a condition known as iron overload may develop from prolonged use of such water with high iron concentrations [10]. Furthermore, consuming too much iron in drinking water can lead to serious health problems like diabetes, cirrhosis, hypothermia, heart failure, and liver damage [10-12]. It may even be linked to many operational problems, such as laundry discoloration, odor, and taste, rendering the water unfit for human use due to aesthetic concerns [8]. All of these concerns therefore demanded immediate attention, which has motivated scientists to reduce the level of Fe pollution. Numerous remediation techniques, including ultrafiltration [13], electrocoagulation [14-18], coagulation flocculation [19], and advanced oxidation [20], and membrane separation [21] are used for eliminating heavy metals. However, there are certain disadvantages to these methods, including low efficiency, the creation of secondary sludge, high running costs, and delicate operating environments [3, 4]. The application of carbonaceous materials as adsorbents for the removal of heavy metals from wastewater has recently become a lucrative area of research [22-24]. Because of its unique structure, prominent surface area, well-developed pore volume, and significant number of active sites for the adsorption of heavy metal ions, activated carbon (AC) is recognized as an efficient and environmentally benign adsorbent [25-27]. Although commercial AC is one of the most popular adsorbents for removing heavy metals from wastewater, its usage is occasionally restricted because of its greater cost [3, 28]. Ultimately, peat, coal, lignite, and wood are used to synthesis AC, which is costly, highly exhaustible, and seen as an annoyance [29].

This circumstance has led numerous researchers to investigate less expensive carbonaceous based materials for the production of activated carbon from biomass derived from cellulose, lignin, and hemicelluloses [30-32]. Indeed, agriculture waste disposal being widely accessible including walnut shell [33], wood sawdust [34], coconut shell [25], cotton cakes [28], lemon peel [35], pecan shell [11], corn cob [6], xhanthoceras sorbifolia [29], jatropha shell [36] and, rice husk [37], etc. have been examined.

Every year, garbage from desert date seed shells appears all over the planet. These waste byproducts directly contribute to pollution in the environment. Therefore, it is crucial to convert agricultural wastes, namely the shell of desert date seeds, into sustainable carbon-based materials in order to reduce pollution in the environment. Furthermore, it can stimulate the economy by efficiently converting these natural resources into a few highly valuable byproducts. In this present work, the AC was synthetized from desert date seed shell which was used to employed to remove iron from aqueous solutions.

AC with a large surface area and a strong ability to adsorb metal ions can be produced by H_3PO_4 or KOH activation of several lignocellulosic compounds [6, 11, 24]. Therefore, the aim of this work is: (i) to assess the potential production of AC from desert date seed shells with phosphoric acid activation and potassium hydroxide; (ii) to determine the properties of the as synthesized AC; (iii) to investigate the ability of the activated carbon to absorb iron (II) present in aqueous solutions.

2. Material and Methods

2.1. Preparation of Adsorbents

Several carbonaceous materials can be chemically or physically activated to create activated carbon. The physical activation was accomplished in an inert atmosphere at temperatures between 800 ℃ and 1100 ℃ [39]. Contrary to physical activation, the chemical activation required low temperature and higher product yield includes single stage that needs the impregnation of the precursor using activating agent like $ZnCl_2$, NH_3, KOH, and H_3PO_4 [23, 25, 32].

The desert date seed shell collected from Ka é, farth nord

region of Cameroon and dried at 45 ℃ in the oven after washing with distilled water [38]. After drying, the samples were crushed and sieved (1 mm), a part is subjected to chemical phosphoric acid (DDSSA) and potassium hydroxide (DDSSS) activations. The beast powders were impregnated with a phosphoric acid and soda solution at room temperature. They were then rinsed with distilled water at a neutral pH and dried using constant weight at 40-50 ℃ and 105 ℃, respectively.

2.2. Preparation of Fe^{2+} Solution

Iron is positively charged heavy metal whose density exceeds 5 g/mL. The stock solution of Fe^{2+}, 1000 mg/L, was prepared from iron (II) sulfate salt heptahydrate $FeSO_4.7H_2O$.

2.3. Adsorbent Characterization

It is able to ascertain the residual humidity of our materials through the water content, while the dry matter gives information on the actual mass of material brought into contact with the solution. As for the ash tenor, it allows to know the mineral, inert and unusable portion of the desert date seed shell.

The relative measure of an adsorbent's porosity is the Iodine Index. It gauges the amount of micropores that tiny molecules can enter and pass through; it was identified by the method used by Faouzia et al. [18].

The functional groups contained in the materials were identified using the Fourier Transform Infra-Red technique. The ball was created by mixing potassium bromide with a pattern, and it was scanned in the 400-4000 cm^{-1} wave-number range. The DDSSA and DDSSS were characterized using field emission scanning electron microscopy (FE-SEM) to determine their structure and morphology. Carl Zeiss Supra 55VP microscope equipped with an accelerating voltage of 0.1-30 kV was used for this purpose.

Laser Raman microscope (LabRam HR, Horiba) with 600 nm wavelength was used to carry out Raman measurements. The spectra were recorded from 1000 and 3000 cm^{-1}. X-ray diffraction (XRD) has been utilized to ascertain the adsorbents' phase purity, grain size, and lattice spacing increase. It is frequently employed in the investigation of DDSSA and DDSSS crystal defects. The XRD patterns of all the samples were measured using Bruker D8 Advance X-ray Diffractometer with rat of 5°/min at λ=1.55 Å in the interval from 5 to 80 °.

The pH_{PZC} plays a key function in determining the precise charge carried by the adsorbent's surface throughout the dye fixing process. This means that the surface's resulting charges, both positive and negative, are equal to zero, or the medium's pH value. For this, 0.2 g of the adsorbents was put in contact with 50 mL of 0.01 M NaCl for pH which will be adjusted by adding NaOH or HCl from 2 to 12 according to Mahmood method [40]. The bottle were closed and stirred at room temperature for 48 hours in order to raise their final pH. The pattern of interception of the final pH (pHf) according to the initial pH (pHi) with bisector determines the pH_{PZC}.

In order to determine the equilibrium pH, 1 g of the adsorbent is dissolved in 100 mL of distilled water (pH = 5.2 ± 0.2), agitated for 24 hours, then allowed to stabilize. A pH-meter (VOLTCRAFT) is then used to collect readings after 25 minutes.

2.4. Adsorption Experiments

The adsorption process was carried out in a batch system by combining 0.01 g of adsorbent with 50 mL of dye solutions at the desired concentration. The mixture was then agitated at 300 rpm for the specified duration at room temperature (25 ± 2 ℃). Whatman filter paper was then used to filter the mixture so that the residual iron (II) concentration could be determined using a UV-visible spectrophotometer (RAYLEIGH). Different mass (0.01-0.1 g), concentration (10-40 mg/L), times (5-40 min), temperatures (298, 308, 318, and 328 K), and pH values (3-11) were used in the experiments. The quantity of dyes adsorbed per mg/g for DDSSA and DDSSS at equilibrium, qe (mg/g), was expressed by equation (1) as follows [41]:

$$qe(mg/g) = \frac{(Ci-Ce)\times V}{m} \quad (1)$$

Where Co = initial concentration (mg/L), Ce = concentration at equilibrium (mg/L), V = volume used (L) and m = mass used (g).

Langmuir Adsorption Isotherm

The Langmuir model implies that the surfaces of the carbonaceous is homogeneous in terms of energy and does not take into account the interactions between the adsorbed molecules. Its equation is as follows:

$$\frac{Ce}{qe} = \frac{Ce}{qmax} + \frac{1}{KL.qmax} \quad (2)$$

Where Ce is the equilibrium concentration of the adsorbate (mg/L); qe is the quantity of adsorbed at equilibrium (mg/g); qmax represent the maximum adsorption capacity (mg/g) and K_L is the Langmuir isotherm constant (L/mg).

Ce/qe in function of Ce gives a straight line with 1/qo a slope and 1/qmax. KL as ordinate axis. To know if the adsorption is linear, irreversible and favorable or not, equilibrium parameter RL was calculated by equation 3:

$$RL = \frac{1}{1+KL.Co} \quad (3)$$

Where Co is the greatest initial concentration of dye (mg L^{-1}) $0 < R_L < 1$: favor adsorption; RL = 1: linear; RL = 0: irreversible and when RL > 1: unfavorable.

Freundlich Adsorption Isotherm

Freundlich assumes that the adsorbent has a heterogeneous surface and that the distribution of active sites is exponential in relation to the adsorption energy. Its equation is represented

as follows (4):

$$\log qe = \frac{1}{n} \log Ce + \log KF \quad (4)$$

Where qe represent the quantity adsorbed at equilibrium (mg/g); Ce is the equilibrium concentration of the adsorbate (mg/L); K_F is the Freundlich constant and n is the constant related to intensity of adsorption associated with heterogeneity factor.

The plots of log qe against log Ce should give a linear graph n = slope; K_F is the intercept of the graph.

Temkin Adsorption Isotherm

This model takes into account the non-uniformity of the surface and the preferential occupation of the spots that are highly adsorbent.

The following situations typically employ the Temkin isothermal model (5):

$$qe = \frac{RT}{b} \ln (A\,Ce) \text{ or } qe = B\ln A + B\ln C \quad (5)$$

With B = RT/b,

Where qe is the quantity adsorbed at equilibrium (mg/g), Ce is the equilibrium concentration of the adsorbate (mg/L); T is the temperature (K), R is the gas constant (8.314 J/mol/K), B and A are calculated from the slope (B) and intercept (B lnA) of the plot of qe against lnCe.

Dubinin-Radushkevic Adsorption Isotherm

It is based on volume filling using Polanyi's potential theory, which postulates that the adsorbate volume is a function of the potential of this field ε and that the contacts between the adsorbate and the adsorbent are established by a potential field.

The Dubinin-Redushkevich equation has the following expression (6):

$$\ln q_e = \ln q_o - \beta\, \varepsilon^2 \quad (6)$$

With q_e (mg/g): quantity of Fe^{2+} adsorbed; β: relative constant of the adsorption energy, q_m: theoretical capacity of the micropores, ε is the potential of Polanyi (ε: RTln (1+1/Ce)).

The kinetic adsorption process was explained by the use of intra-particle diffusion as well as pseudo-first and second-order diffusion. Lagergren has proposed this equation (7):

$$\log (qe - qt) = \log qe - \frac{t}{2.303} K1 \quad (7)$$

Where K_1= the rate constant (min^{-1}), qe = quantity adsorbed on surface at equilibrium (mg/g), and qt = quantity adsorbed on surface at time (mg/g).

Equation 8 is that of the 2nd order kinetic:

$$\frac{t}{qt} = \frac{1}{K2qe^2} + \frac{1}{qe} t \quad (8)$$

K_2 (mg/g.min) = 2nd order rate constant

The Weber-Morris intraparticle diffusion model is determined using the following equation 9:

$$qt = K_3 t^{1/2} + C' \quad (9)$$

Where K_3 is the intraparticle diffusion rate constant ($mg/g.min^{-1/2}$) and C' is the intercept.

The following Van't Hoff equations were used to calculate thermodynamic characteristics, such as free standard energy ΔG° (Kj/mol), standard enthalpy ΔH° (Kj/mol), and standard entropy (ΔS°) (Kj/mol/K), through adsorption at three distinct temperatures:

$$\Delta rG° = -RT\ln Kc \quad (10)$$

$$Kc = \frac{qe}{Ce} \quad (11)$$

$$\ln Kc = \frac{\Delta rS°}{R} - \frac{\Delta rH°}{RT} \quad (12)$$

Where Kc is the equilibrium constant; qe (mg/g) is the quantity adsorbed; Ce (mg/L) represente the concentration of solution at equilibrium; R is the gas constant (8.314 J/mol/K); and T is the temperature (K).

3. Results and Discussion

3.1. Characterizations of Adsorbent

Figure 1 displays FE-SEM micrographs of DDSSA and DDSSS. Compared to DDSS, DDSSA has a more porous and highly uneven rough structure in the shape of a mound; as a result, a higher adsorption capacity is justified by a greater specific area [42]. The specific area of DDSS and DDSSA are 55.47 and 75.74 $m^2.g^{-1}$, respectively.

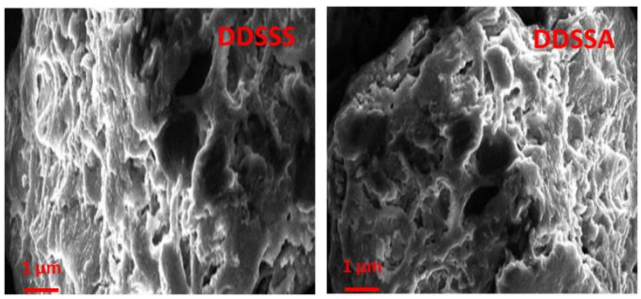

Figure 1. *FE-SEM micrographs of DDSSS and DDSSA.*

Figure 2 displays the outcome of using FTIR to identify any functional groups that may be present. The infrared spectra of the material show two distinct peaks that represent DDSSS and DDSSA, five comparable stretching vibration peaks, and one deformation vibration. Due to the acidic nature of our desert date seed shell, we first have a sweeping tape in the

region of 3567 - 3118 cm^{-1} assigned to the O-H (carboxyl, phenol, or alcohol) for similar peaks. Second, the aliphatic C-H vibration is characterized by the band seen at 2916 cm^{-1}. Thirdly, the strip at 1731 cm^{-1} suggests that carboxylic acids, esters, ketones, and aldehydes have carbon atoms attached to them. Fourth, the aromatic C=C-corresponding strip in the 1625-1521 cm^{-1} region. The fifth and final strip is 1033 cm^{-1}, which is supposed to represent the C-C bond, and 751 cm^{-1}, which corresponds to the deformation shudder of an aromatic C-H bond that is di- or tri-substituted. These findings are typically consistent with the literature. [43-45].

As a result of reflection in the graphitic structure's plane, the XRD pattern (figure 2) revealed the diffraction peaks 2θ for DDSSS and DDSSA at 25.51 ° and 25.01 °, respectively. An important characteristic for very porous materials is the peak at 42 °, which is attributed to (100), which indicates a lesser degree of graphitization and a larger degree of disorder [34, 46, 47]. Other researchers have already made similar observations [45, 48].

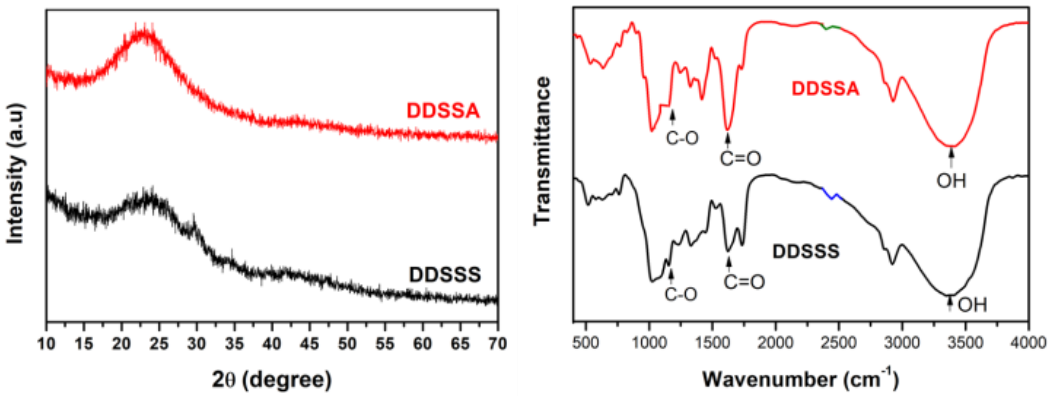

Figure 2. *a) XRD and b) spectrum of DDSSA and DDSSS.*

Figure 3 presents the results of the evaluation of the vibrational properties of the materials using Raman Spectroscopy. Three main peaks are observed in both materials at 1348, 1598, and 2670 cm^{-1}, which correspond to the bands D, G, and 2D, respectively. A defect or disorder in the material's carbon is indicated by the D-band, sp^2 carbon hybridization is indicated by the G-band, and double Raman scattering, or the emission of two photons, is indicated by the 2D-band [49]. The degree of defect or disorder in materials is estimated using the band intensities ratio I_D/I_G. The values of ratio I_D/I_G of DDSSA (0.918) is small than that of DDSSS (0.954) indicating that this AC contain less defect/disorder.

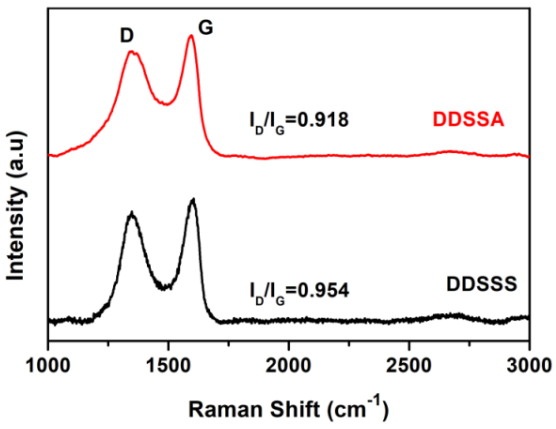

Figure 3. *Raman Spectroscopy of DDSSA and DDSSS.*

Table 1. *Dry matter, moisture and ash tenor of DDSSA and DDSSS.*

Adsorbents	Dry Matter (%)	Moisture content (%)	Ash content (%)
DDSSA	73.21 ±4.90	26.79 ±4.90	0.13 ±0.08
DDSSS	49.19 ±0.81	50.81 ±0.81	0.16 ±0.12

This table shows that DDSSA has the highest dry matter content and the lowest moisture and ash concentrations. The reduced ash level of both adsorbents makes them a better choice than those acquired by Vunain et al. in 2017 [50], and low ash content indicates a good adsorbent.

Table 2. *Specific area, iodine indices, equilibrium pH and pH_{zpc} of DDSSA and DDSSS.*

Adsorbents	Specific Area (m^2/g)	Iodine index (mg/g)	pH	PHzpc
DDSSA	65.74	468.28 ±5.38	5.60 ±0.03	6.89
DDSSS	49.70	441.63 ±0.00	4.86 ±0.02	4.51

DDSSA has a higher specific surface value than DDSSS. We may conclude that the porous structure of our samples has

minimal effect on the adsorption properties based on the values of specific surface. The valor of equilibrium pH of DDSSA and DDSSS are acid; this is due to the way each support has been made.

3.2. Effect of Contact Time and Initial Concentration

In order to investigate how contact time and the initial concentration of Fe^{2+} affect the dye solutions' ability to remove Fe^{2+}, tests were conducted at a fixed mass (0.01 g), pH 6.60 for Fe^{2+} at varying concentrations (10-40 mg/L), and intervals of time (5-40 minutes). It can be shown that the amount removed augments with concentration and that the plateau formation time is independent of concentration. Figure 4 illustrates how quickly adsorption occurs for the first 20 minutes of thermally treated support and the first 15 minutes of chemically treated support with soda and acid before a plateau forms and saturation tends to occur. This can be justified by the fact that there is initially a larger rate of adsorption because the adsorption sites are unoccupied, and later the adsorption rate decreases because the materials' pores are clogged and are saturated by the dissolved species. The increase in the initial adsorption rate with the starting concentration is attributed to the force of attraction between molecules and adsorption sites, and it is greater for DDSSA (122.25 mg/g) than for DDSSS (116.35 mg/g). Furthermore, any resistant mass transfer between the species of aqueous solution and the portion of the adsorbent material is strongly forcefully supported by the initial concentration [51]. These values are superior to those gained by Domga et al [52] 12.67 mg/g for a concentration of 60 mg/g.

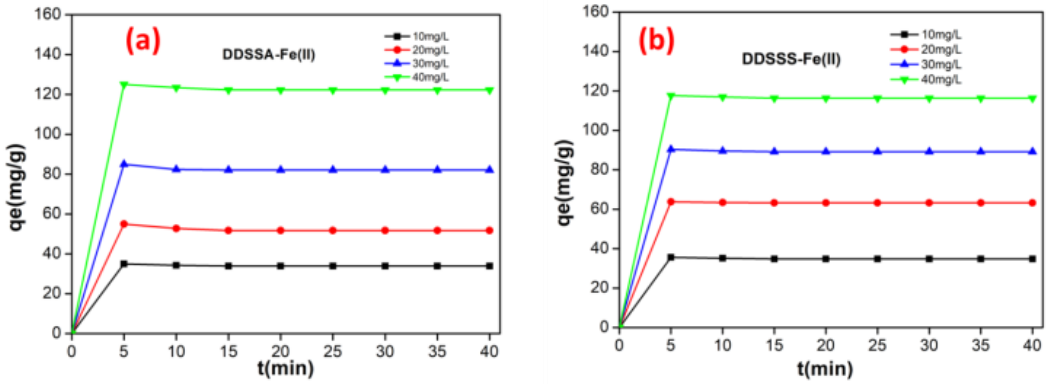

Figure 4. *Effect of contact time and concentration on adsorption capacity of Fe (II) (initial concentration of Fe (II) 10 mg/L, adsorbent dose 0.01g, pH 6.60).*

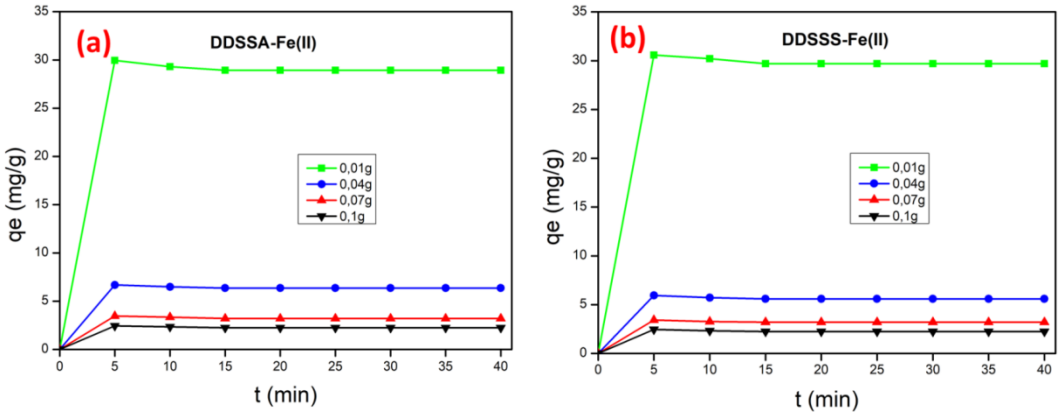

Figure 5. *Effect of Adsorbent Mass on adsorption capacity of Fe (II) (initial concentration of Fe (II) 10 mg/L, pH 6.60).*

3.3. Effect of Adsorbent Mass

Figure 5 shows that, regardless of the adsorbent used, the adsorbed amount of Fe^{2+} decreases with increased mass (24.94-2.25 mg/g and 25.58-2.23 mg/g for DDSSA and DDSSS, respectively). This is because the adsorbent's small sites causes the adsorbent to desorb, and the unsaturation of adsorption sites and reciprocal influence between molecules causes this to happen [33]. Similar observations are obtained by Wu et al. [53]. It can be concluded that DDSSS removed more Fe (II) than DDSSA and the optimum mass of both

adsorbents is 0.01 g and this value was used for the rest of the investigation.

3.4. Effect of Temperature

Figure 6 is a study of the impact of temperature. Based on these curves, it can be assumed that the adsorption of Fe^{2+} onto DDSSS and DDSSA is exothermic because it drops as the temperature rises. For example when the temperature increases from 25 to 55 ℃ the adsorption of Fe(II) onto DDSSS and DDSSA drops from 24.43 to 20.07 mg/g and from 27.64 to 25.33 mg/g, respectively. Since a sizable portion of the microspores with the same dimensions as the molecule can only pass through these pores at specific temperatures, the pore size is responsible for this drop in the amount adsorbed [54].

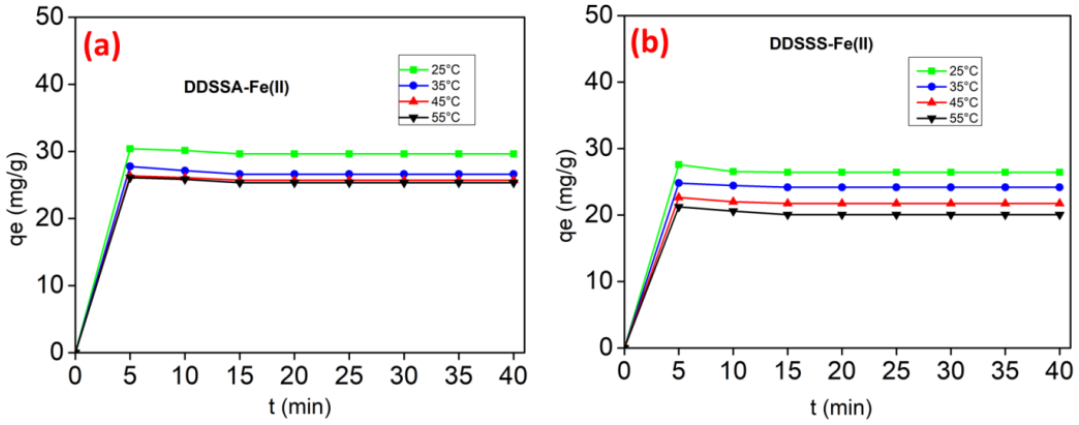

Figure 6. *Effect of temperature on adsorption capacity of Fe (II) (initial concentration of Fe (II) 10 mg/L, adsorbent dose 0.01g, pH 6.60).*

3.5. Effect of PH

Because it affects both the potential charges on the adsorbents' surfaces and the forms of the elements adsorbed in solution, pH is a crucial variable to monitor during the adsorption process [45, 54]. As shown in figure 7, it can be show that when the pH rises, the adsorbed quantity of Fe^{2+} drops at optimal pH 3 and DDSSS (32.12 mg/g) removed more Fe^{2+} in solution than DDSSA (27.25 mg/g). The surface of DDSSA and DDSSS are positively charged because the pH < pHpzc.

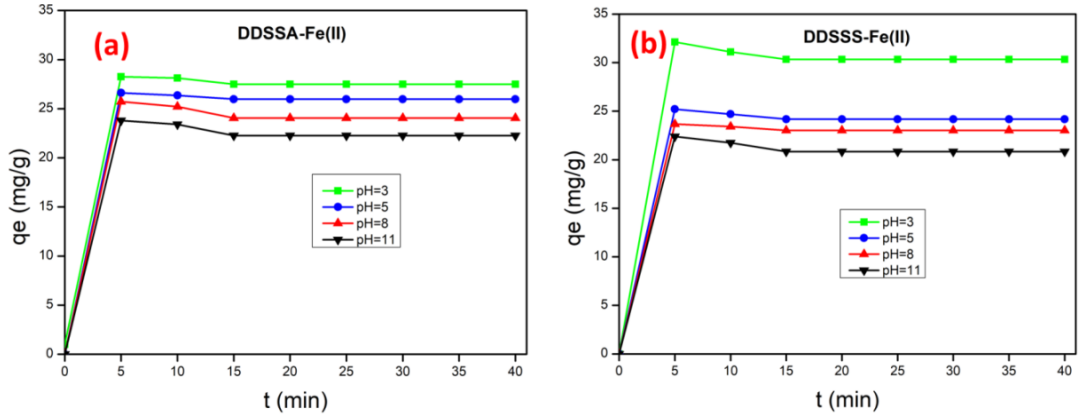

Figure 7*. Effect of pH on adsorption capacity of Fe (II) (initial concentration of Fe (II) 10 mg/L, adsorbent dose 0.01g).*

3.6. Adsorption Isotherm

Four appropriate model isotherms Langmuir, Freundlich, Temkin, and Dubinin-Redushkevic were utilized to quantify the adsorbate-adsorbent interaction and the results are summarized in Table 3.

These analyses (Table 3) indicates that only Freudlich and Temkin isothermal can only be best explained the phenomenon of Fe^{2+} removal onto DDSSA and DDSSS adsorbent.

Table 3. Langmuir, Freundlich, Temkin and Dubinin-Radushkevic on adsorption capacity of Fe (II) (initial concentration of Fe (II) 10 mg/L, adsorbent dose 0.01g).

Isotherms	Parameters	DDSSA	DDSSS
Langmuir	q_{max} (mg/g)	-126.000	-334.333
	K_L (L/mg)	-0.031	-0.017
	R^2	0.950	0.175
Freundlich	N	0.706	0.830
	K_F (mg/g)	2.217	4.307
	R^2	0.984	0.905
Temkin	B	-54.067	-63.545
	A	0.069	0.81
	R^2	0.999	0.999
Dubinin-Radushkevic	Qo	$2.2\ 10^{34}$	$1.9\ 10^{-08}$
	B	0.0003	-0.0009
	R^2	0.015	0.863

3.7. Adsorption Kinetics

The characteristics of the Intraparticular scattering kinetic model such as K_1, K_1 and qe are calculated and listed in Table 4.

Based on the data below, it can be concluded that only the pseudo-2nd model—whose mechanism involves two steps—best explains the adsorption of Fe^{2+}. This is because the value of correlation coefficients R^2 is greater than 0.90 and the Fe^{2+} diffuses to the area and interacts with the Fe^{2+} molecules in the adsorbent area.

Table 4. Pseudo-first order, pseudo-second and intra-particle diffusion kinetic models obtained for Fe(II) adsorption.

Models	Parameters	DDSSA	DDSSS
Pseudo-first-order	R^2	0.315	0.516
	K_1 (min^{-1})	-0.053	-0.031
	qe_{cal} (mg/g)	0.414	0.801
Pseud-second-order	R^2	0.999	0.999
	K_2 (mg/g. min)	-0.492	-0.474
	qe_{cal} (mg/g)	24.809	25.630
Intra-particle Diffusion	R^2	0.637	0.639
	K_3(mg/g. $min^{-1/2}$)	$7.58\ 10^{02}$	$2.08\ 10^{03}$
	C’	4.44 1009	7.52 1009

3.8. Thermodynamics Parameters

Table 5 presented a summary of the thermodynamics parameters results.

Table 5. The thermodynamics parameters for the adsorption of Fe^{2+} by DDSSA and DDSSS.

Adsorbent	ΔrH° (Kj/mol)	ΔrS° (Kj/mol)	R^2	ΔrG° (Kj/mol)			
				298	308	318	328
DDSSA	-2.227	-0.0009	0.974	-1.959	-1.933	-1.913	-1.937
DDSSS	-4.410	-0.008	0.915	-2.278	-2.355	-2.431	-2.508

Table 5 shows that the enthalpy parameter ΔH° (KJ/K. mol) is negative. This suggests that Fe^{2+} elimination is exothermic, and the reaction is physical in nature and spontaneous, with all ΔrG° values being negative. Regarding the values of ΔrS°, we can state that there is a reduction at the DDSSA and DDSSS interface, which results in good Fe^{2+} organization at the adsorption site level.

4. Conclusion

In order to remove Fe^{2+} from an aqueous solution, this study examined the use of inexpensive adsorbents made from desert date seed shell enabled potassium hydroxide (DDSSS) and phosphoric acid (DDSSA). The presence of functional groups necessary for the removal of Fe^{2+} by DDSSA and DDSSS was discovered through the surface characterization of adsorbents. SEM micrographs revealed porous structures with distinct chemical functionalities on their surfaces based on how they are activated. The amount adsorbed increases with concentration and decreases with mass, temperature, and pH, according to a study of several parameters throughout time, including initial concentration, mass, temperature, and

pH. The Fe^{2+} adsorption process was better described by the pseudo 2nd order model and the Freundlich and Temkin isotherm than by Langmuir and Dubinin-Radushkevich. Furthermore, the spontaneous, physical type, and exothermic nature of the adsorption process was confirmed by thermodynamics. The study's conclusions can be summed up as follows: low-coast adsorbents (DDSSA and DDSSS) effectively remove Fe^{2+} contaminants. Additional dyes can be removed from different aqueous solutions using the methodology described in this study.

Abbreviations

pH	Potential of Hydrogen
Fe	Iron
DDSSA	Desert Date Seed Shell Enabled Phosphoric Acid
DDSSS	Desert Date Seed Shell Enabled Potassium Hydroxide
SEM	Scanning Electron Microscopy
XRD	X-ray Diffraction
FTIR	Fourier Transform Infra-Red Technique

Author Contributions

Benessoubo Kada Danièle: Data curation, Methodology, Writing - original draft

Domga: Conceptualization, Formal Analysis, Methodology, Project administration, Supervision, Writing - original draft, Writing - review & editing

Yanu Asobo Celestine: Formal Analysis, Investigation, Methodology, Writing - review & editing

Taybe Ngaba: Formal Analysis, Methodology, Writing - review & editing

Kowe Jean Olivier: Formal Analysis, Investigation, Writing - original draft

Conflicts of Interest

The authors declare no conflicts of interest.

References

[1] K. H. Hama Aziz, F.S. Mustafa, K.M. Omer, S. Hama, R.F. Hamarawf, K.O. Rahman. 2023. "Heavy metal pollution in the aquatic environment: efficient and low-cost removal approaches to eliminate their toxicity: a review. " RSC Adv. 13 17595-17610. https://doi.org/10.1039/d3ra00723e

[2] Aloulou, Wala, Hajer Aloulou, Mouna Khemakhem, and Joelle Duplay. 2020. "Environmental Technology & Innovation Synthesis and Characterization of Clay-Based Ultrafiltration Membranes Supported on Natural Zeolite for Removal of Heavy Metals from Wastewater." Environmental Technology & Innovation 18: 100794. https://doi.org/10.1016/j.eti.2020.100794

[3] Vasudevan, Subramanyan and Lakshmi, Jothinathan. 2012. "Process Conditions and Kinetics for the Removal of Copper from Water by Electrocoagulation" Environmental Engineering Science 29 (7). https://doi.org/10.1089/ees.2010.0429

[4] Astuti, Widi, Triastuti Sulistyaningsih, Ella Kusumastuti, Gui Yanny, and Ratna Sari. 2019. "Bioresource Technology Thermal Conversion of Pineapple Crown Leaf Waste to Magnetized Activated Carbon for Dye Removal." Bioresource Technology 287: 121426. https://doi.org/10.1016/j.biortech.2019.121426

[5] Bembli, Meriem, Mohamed Zine, Ali Bechrifa, and Khaled Boughzala. 2022. "Study of the Adsorption of Acid Red 52 by By-Products of the Phosphate Industry." RHAZES: Green and Applied Chemistry 15: 51-65.

[6] Benaïssa, H, and M A Elouchdi. 2011. "Biosorption of Copper (II) Ions from Synthetic Aqueous Solutions by Drying Bed Activated Sludge." Journal of Hazardous Materials Journal 194: 69-78. https://doi.org/10.1016/j.jhazmat.2011.07.063

[7] Campos, Natália F., A Giovanna, Leticia P S Oliveira, Brígida M. V. Gama, Deivson C. S. Sales, M Joan, Celmy M. B. M. Barbosa, and M M B Marta. 2020. "Competitive Adsorption between Cu_2+ and Ni_2+ on Corn Cob Activated Carbon and the Difference of Thermal Effects on Mono and Bicomponent Systems." Journal of Environmental Chemical Engineering 8 (5): 104232. https://doi.org/10.1016/j.jece.2020.104232

[8] Chen, Hao, Yao Jun Zhang, Pan Yang He, Chan Juan Li, and Huan Li. 2020. "Applied Surface Science Coupling of Self-Supporting Geopolymer Membrane with Intercepted Cr (III) for Dye Wastewater Treatment by Hybrid Photocatalysis and Membrane Separation." Applied Surface Science 515 (13): 146024. https://doi.org/10.1016/j.apsusc.2020.146024

[9] Chukwuemeka, Helen O, Okorie Francis, K Ekuma Kovo, Jude C Nnaji, and Amarachi G Okereafor. 2021. "Adsorption of Tartrazine and Sunset Yellow Anionic Dyes onto Activated Carbon Derived from Cassava Sievate Biomass." Applied Water Science 11 (27): 1-8. https://doi.org/10.1007/s13201-021-01357-w

[10] Daouda, Abia, Amana Tokodne Honorine, Noumi Guy Bertrand, and Domga Richard. 2019. "Adsorption of Rhodamine B onto Orange Peel Powder." American Journal of Chemistry 9 (5): 142-49. https://doi.org/10.5923/j.chemistry.20190905.02

[11] Daouda, Abia, Yowe Kidwe, Domga Richard, and Harouna Massai. 2019. "Adsorption of Cu 2 + and Cr 6 + in Aqueous Solution by a Thermally Modified Biosorbent Based on Cotton Cakes" American Journal of Physical Chemistry 8 (4): 66-74. https://doi.org/10.11648/j.ajpc.20190804.11

[12] Das, Shilpi, and Susmita Mishra. 2020. "Insight into the Isotherm Modelling, Kinetic and Thermodynamic Exploration of Iron Adsorption from Aqueous Media by Activated Carbon Developed from Limonia Acidissima Shell." Materials Chemistry and Physics 245 (January): 122751. https://doi.org/10.1016/j.matchemphys.2020.122751

[13] Dawood, Sara, Tushar Kanti Sen, and Chi Phan. 2017. "Synthesis and Characterisation of Slow Pyrolysis Pine Cone Bio-Char in the Removal of Organic and Inorganic Pollutants from Aqueous Solution by Adsorption : Kinetic, Equilibrium, Mechanism and Thermodynamic." Bioresource Technology 246: 76-81. https://doi.org/10.1016/j.biortech.2017.07.019

[14] Domga, R, C Tcheka, G Mouthe, N Kobbe, and J Tchigo Tchatchueng. 2016. "Batch Equilibrium Adsorption of Methyl Orange from Aqueous Solution Using Animal Activated Carbon from Gudali Bones." International Journal of Innovation Sciences and Research 5 (7): 798-805.

[15] Dubinin, M. M. and Radushkevich, L. V. 1947. "Equation of the Characteristic Curve of Activated Charcoal." Proc. Acad. Sci. Phys. Chem. USSR 55: 331-333.

[16] El-azazy, Marwa, and Ahmed S El-shafie. 2021. "Biochar of Spent Coffee Grounds as Per Se and Impregnated for Balofloxacin." Molecules 26 (2295): 1-22.

[17] Ernesto, De La Torre. 2015. "Préparation de charbon actif à partir de coques de noix de palmier à huile pour la récupération d'or et le traitement d'effluents cyanurés. " Thesis Université Catholique de Louvain

[18] Faouzia Benamraoui. 2014. "Elimination of Cationic Dyes by Activated Carbons Synthesized from Agricultural Residues."Thesis Ferhat Abbas Setif University 1-103.

[19] Güzel, Fuat. 2018. "Novel and Sustainable Precursor for High-Quality Activated Carbon Preparation by Conventional Pyrolysis : Optimization of Produce Conditions and Feasibility in Adsorption Studies." Advanced Powder Technology journal 29 (3) 726-736. https://doi.org/10.1016/j.apt.2017.12.014

[20] Habaki, Hiroaki, Tomoki Hayashi, Patima Sinthupinyo, and Ryuichi Egashira. 2019. "Purification of Glycerol from Transesteri Fi Cation Using Activated Carbon Prepared from Jatropha Shell for Biodiesel Production." Journal of Environmental Chemical Engineering 7 (5): 103303. https://doi.org/10.1016/j.jece.2019.103303

[21] Haddad, Khouloud, Salah Jellali, Safa Jaouadi, and Mahmoud Benltifa. 2014. "Raw and Treated Marble Wastes Reuse as Low Cost Materials for Phosphorus Removal from Aqueous Solutions : Efficiencies and Mechanisms." Comptes Rendus Chimie, 1-13. https://doi.org/10.1016/j.crci.2014.07.006

[22] Ho, Y. S and Mckay, G. 1998. "A Comparison of Chemisorption Kinetic Models Applied to Pollutant Removal on Various Sorbents." Proc. Saf. Environ. Protec. 76: 332-340.

[23] Jagadeesh, Alagarasan, Rajendra Prasad, Dafang Fu, and Chinnaiya Namasivayam. 2017. "Comparison of Physical- and Chemical- Activated Jatropha Curcas Husk Carbon as an Adsorbent for the Adsorption of Reactive Red 2 from Aqueous Solution." Desalination and Water Treatment 95: 308-18. https://doi.org/10.5004/dwt.2017.21255

[24] Kalagatur, Naveen K, Kumarvel Karthick, Joseph A Allen, Oriparambil Sivaraman, Nirmal Ghosh, Siddaiah Chandranayaka, and Vijai K Gupta. 2017. "Application of Activated Carbon Derived from Seed Shells of Jatropha Curcas for Decontamination of Zearalenone Mycotoxin" 8 (October): 1-13. https://doi.org/10.3389/fphar.2017.00760

[25] Kamaraj, Ramakrishnan, and Pandian Ganesan. 2013. "Removal of Copper from Water by Electrocoagulation Process — Effect of Alternating Current (AC) and Direct Current (DC)" Environmental Science and Pollution Research 20 399-412. https://doi.org/10.1007/s11356-012-0855-7

[26] Kaveeshwar, Aditya Rajeev, SenthilKumar Ponnusamy, Emmanuel D Revellame, Daniel D Gang, E Zappi, and Ramalingam Subramaniam. 2018. "Pecan Shell Based Activated Carbon for Removal of Iron (II) from Fracking Wastewater: Adsorption Kinetics, Isotherm and Thermodynamic Studies." Process Safety and Environmental Protection 114: 107-22. https://doi.org/10.1016/j.psep.2017.12.007

[27] Kaya, Nihan, Ferhat Arslan, Zeynep Yıldız Uzun, and Selim Ceylan. 2020. "Kinetic and Thermodynamic Studies on the Adsorption of Cu 2+ Ions from Aqueous Solution by Using Agricultural Waste-Derived Biochars." Water Supply 20 (8): 3120-40. https://doi.org/10.2166/ws.2020.193

[28] Khatri, Nitasha, Sanjiv Tyagi, and Deepak Rawtani. 2017. "Journal of Water Process Engineering Recent Strategies for the Removal of Iron from Water : A Review." Journal of Water Process Engineering 19 (13): 291-304. https://doi.org/10.1016/j.jwpe.2017.08.015

[29] Kim, Taeyeon, Tae-kyoung Kim, and Kyung-duk Zoh. 2020. "Journal of Water Process Engineering Removal Mechanism of Heavy Metal (Cu, Ni, Zn, and Cr) in the Presence of Cyanide during Electrocoagulation Using Fe and Al Electrodes." Journal of Water Process Engineering 33 (July 2019): 101109. https://doi.org/10.1016/j.jwpe.2019.101109

[30] Lagergren, S. and Svenska, B. K. 1898. "On the Theory of So-Called Adsorption of Materials." R. Swed. Acad. Sci. Doc., Band. 24: 1-13.

[31] Li, Yiran, Jian Zhang, and Hai Liu. 2018. "In-Situ Modi Fi Cation of Activated Carbon with Ethylenediaminetetraacetic Acid Disodium Salt during Phosphoric Acid Activation for Enhancement of Nickel Removal." Powder Technology 325: 113-20. https://doi.org/10.1016/j.powtec.2017.10.051

[32] Liang, Jialin, Liang Zhang, Maoyou Ye, Zhijie Guan, Jinjia Huang, and Jingyong Liu. 2020. "Evaluation of the Dewaterability, Heavy Metal Toxicity and Phytotoxicity of Sewage Sludge in Different Advanced Oxidation Processes." Journal of Cleaner Production 265: 121839. https://doi.org/10.1016/j.jclepro.2020.121839

[33] Liu, Xin, Changquan He, Xingjian Yu, Yuting Bai, Ling Ye, Bangsen Wang, and Lingfan Zhang. 2018. "Net-like Porous Activated Carbon Materials from Shrimp Shell by Solution-Processed Carbonization and H_3PO_4 Activation for Methylene Blue Adsorption." Powder Technology 326: 181-89. https://doi.org/10.1016/j.powtec.2017.12.034

[34] Ma, Jianqing, Yu Shen, Chensi Shen, Yuezhong Wen, and Weiping Liu. 2014. "Al-Doping Chitosan - Fe (III) Hydrogel for the Removal of Fluoride from Aqueous Solutions." Chemical Engineering Journal 248: 98-106. https://doi.org/10.1016/j.cej.2014.02.098

[35] Maguana, Y El, N Elhadiri, M Bouchdoug, M Benchanaa, and A Jaouad. 2019. "Activated Carbon from Prickly Pear Seed Cake: Optimization of Preparation Conditions Using Experimental Design and Its Application in Dye Removal" 2019.

[36] Mahmood, Tahira, Muhammad Tahir Saddique, Abdul Naeem, Paul Westerho, and Syed Mustafa. 2011. "Comparison of Different Methods for the Point of Zero Charge Determination of NiO." Industrial & Engineering Chemistry Research 50: 10017-23.

[37] Massai, Harouna, Djakba Raphael, and Mouhamadou Sali. 2020. "Adsorption of Copper Ions (Cu ++) in Aqueous Solution Using Activated Carbon and Biosorbent from Indian Jujube (Ziziphus Mauritiana) Seed Hulls." Chemical Science International Journal 29 (5): 13-24. https://doi.org/10.9734/CSJI/2020/v29i530177

[38] Meseldžija, Slađana, Jelena Petrović, Antonije Onjia, Tatjana Volkov-husović, Aleksandra Nešić, and Nikola Vukelić. 2020. "Removal of Fe^{2+}, Zn^{2+} and Mn^{2+} from the Mining Wastewater by Lemon Peel Waste." Journal of the Serbian Chemical Society 85 (10): 1371-82.

[39] Peng, Hongbo, Peng Gao, Gang Chu, Bo Pan, Jinhui Peng, and Baoshan Xing. 2017. "Enhanced Adsorption of Cu(II) and Cd(II) by Phosphoric Acid-Modified Biochars." Environmental Pollution, 1-8. https://doi.org/10.1016/j.envpol.2017.07.004

[40] Phuengphai, Pongthipun, Thapanee Singjanusong, and Napaporn Kheangkhun. 2021. "Removal of Copper (II) from Aqueous Solution Using Chemically Modified Fruit Peels as Efficient Low-Cost Biosorbents." Water Science and Engineering 14 (4): 286-94. https://doi.org/10.1016/j.wse.2021.08.003

[41] Rao. M. 2002. Removal of Cr (VI) and Ni (II) from Aqueous Solutions Using Bagasse and Fly Ash, Waste Manage. Vol. 22.

[42] Rotimi, Ayodele, Ipeaiyeda Mohammed, Iqbal Choudhary, and Shakil Ahmed. 2018. "Ammonia and Ammonium Acetate Modifications and Characterisation of Activated Carbons from Palm Kernel Shell and Coconut Shell." Waste and Biomass Valorization 11 (3): 983-993. https://doi.org/10.1007/s12649-018-0414-7

[43] Roy, Swapnila, Papita Das, and Shubhalakshmi Sengupta. 2016. "Treatability Study Using Novel Activated Carbon Prepared from Rice Husk: Column Study, Optimization Using Response Surface Methodology and Mathematical Modeling." Process Safety and Environmental Protection. https://doi.org/10.1016/j.psep.2016.11.007

[44] Sha, Liang, G U O Xue-yi, Feng Ning-chuan, and Tian Qing-hua. 2010. "Effective Removal of Heavy Metals from Aqueous Solutions by Orange Peel Xanthate." Transactions of Nonferrous Metals Society of China 20: 187-91. https://doi.org/10.1016/S1003-6326(10) 60037-4

[45] Domga, M. Karnan, F. Oladoyinbo, G. Bertrand, J. Bosco, M. Joseph, M. Sathish, D.K. Pattanayak. 2020. "A simple, economical one-pot microwave assisted synthesis of nitrogen and sulfur co-doped graphene for high energy supercapacitors." Electrochim. Acta 341: 1-14. https://doi.org/10.1016/j.electacta.2020.135999

[46] Momo, B.Z. Domga, Doumbi, R.T. Motue Waffo, L.C. Noumi, G.B. Tchatchueng, J.B. Synthesis of nitrogen and sulfur bi-doped carbon obtained from spent sapelli wood sawdust and polyhydric alcohol with improved catalytic activity for hydrogen evolution reaction, Results Eng. 22 (2024) 102245. https://doi.org/10.1016/j.rineng.2024.102245

[47] Tumampos, Stephanie B, Benny Marie B Ensano, Sheila Mae B Pingul-ong, Dennis C Ong, Chi-chuan Kan, Jurng-jae Yee, and Mark Daniel G De Luna. 2021. "Isotherm, Kinetics and Thermodynamics of Cu (II) and Pb (II) Adsorption on Groundwater Treatment Sludge-Derived Manganese Dioxide for Wastewater Treatment Applications." International Journal of Environmental Research and Public Health 18 (3050): 1-13.

[48] Domga, T. Bertrand, G. Joseph, M. Bosco. J. 2021. "Synthesis of nitrogen and phosphorus co-doped graphene as efficient electrocatalyst for oxygen reduction reaction under strong alkaline media in advanced chlor-alkali cell. " Carbon Trends 4: 1-12. https://doi.org/10.1016/j.cartre.2021.100043.

[49] Vasudevan, Subramanyan, Jeganathan Jayaraj, Jothinathan Lakshmi, and Ganapathy Sozhan. 2009. "Removal of Iron from Drinking Water by Electrocoagulation: Adsorption and Kinetics Studies" 26 (4): 1058-64. https://doi.org/10.1007/s11814-009-0176-9

[50] Vunain, Ephraim, Davie Kenneth, and Timothy Biswick. 2017. "Synthesis and Characterization of Low-Cost Activated Carbon Prepared from Malawian Baobab Fruit Shells by H3PO4 Activation for Removal of Cu (II) Ions: Equilibrium and Kinetics Studies." Applied Water Science 7 (8): 4301-19. https://doi.org/10.1007/s13201-017-0573-x

[51] Wang, Qiaorui, Chunli Zheng, Wei Cui, Fei He, Jianyu Zhang, Tian C Zhang, and Chi He. 2019. "Adsorption of Pb2+ and Cu2+ Ions on the CS2-Modified Alkaline Lignin." Chemical Engineering Journal, 123581. https://doi.org/10.1016/j.cej.2019.123581

[52] Domga, R., Tcheka, C., Mouthe Anombogo, G. A., Kobbe-Dama, N., Domga, Tchatchueng, J. B., Tchigo, A. & Tsafam, A. 2016. "Batch equilibrium adsorption of methyl orange from aqueous solution using animal activated carbon from Gudali Bones." International Journal of Innovation Sciences and Research 5 (7), 798-805

[53] Wu, Long, Wenjie Wan, Zhongsheng Shang, Xinyuan Gao, Noriyuki Kobayashi, Guangqian Luo, and Zhanyong Li. 2018. "Surface Modification of Phosphoric Acid Activated Carbon by Using Non-Thermal Plasma for Enhancement of Cu(II) Adsorption from Aqueous Solutions." Separation and Purification Technology 197: 156-169 https://doi.org/10.1016/j.seppur.2018.01.007

[54] Zhang, Xiaotao, Yinan Hao, Ximing Wang, and Zhangjing Chen. 2017. "Adsorption of Iron (III), Cobalt (II), and Nickel (II) on Activated Carbon Derived from Xanthoceras Sorbifolia Bunge Hull: Mechanisms, Kinetics and in Fl Uencing Parameters." Water Science and Technology 75 (8): 1849-61. https://doi.org/10.2166/wst.2017.067

Research Field

Benessoubo Kada Daniède: Process design and conception engineering, Valorization of lignocellulosic and natural geological residues, Optimization of industrial processes, Physical chemistry of interfaces, Wastewater treatment

Domga: Synthesis of carbonaceous based materials, Advanced chlor-alkali process, Wastewater treatment, Materials Chemistry, Adsorption, Electrochemical analysis

Yanu Asobo Celestine: Wastewater treatment, Portable water treatment, Material science, Optimization process using experimental design, Formulation engineering (cosmetic, pharmaceutical, bioactive), Process design and conception engineering

Taybe Ngaba: Civil engineering and sustainable construction, Optimization process, Building materials and architecture, Wastewater treatment, Adsorption

Kowe Jean Olivier: Wastewater treatment, Electrochemistry, Material science, Valorization of lignocellulosic and natural geological residues, Adsorption